Proceedings of the 9th U.S. National and 10th Canadian Conference on Earthquake Engineering
Compte Rendu de la 9ième Conférence Nationale Américaine et
10ième Conférence Canadienne de Génie Parasismique
July 25-29, 2010, Toronto, Ontario, Canada • Paper No 1100

EXPERIMENTAL INSIGHT INTO LIQUEFACTION-INDUCED BUILDING SETTLEMENT

S. Dashti[1], J. D. Bray[2], J. M. Pestana[3], M. Riemer[4], and D. Wilson[5]

ABSTRACT

Seismically induced settlement of buildings with shallow foundations on liquefiable soils has resulted in significant damage in recent earthquakes. The state-of-the-practice still largely involves estimating building settlement using empirical procedures developed to calculate post-liquefaction consolidation settlement in the free-field. Geotechnical centrifuge experiments were performed to identify the dominant mechanisms involved in liquefaction-induced building settlement. The centrifuge tests revealed that considerable building settlement occurs during earthquake strong shaking. Volumetric strains due to localized drainage in response to high transient hydraulic gradients and deviatoric strains due to shaking-induced ratcheting of the buildings into the softened soil are important effects that are currently not captured in current procedures (e.g., Tokimatsu and Seed 1987; Ishihara and Yoshimine 1992). The relative importance of each mechanism depends on the characteristics of the earthquake motion, liquefiable soil, and building. The initiation, rate, and amount of liquefaction-induced building settlement depend greatly on the rate of ground shaking, which can be represented by the shaking intensity rate (*SIR*) parameter.

Introduction

The state-of-the-practice for estimating liquefaction-induced building settlement relies heavily on empirical procedures developed to estimate post-liquefaction consolidation settlement in the free-field, without the effects of structures (e.g., Tokimatsu and Seed 1987; Ishihara and Yoshimine 1992). Estimating building settlement based on free-field, post-liquefaction, reconsolidation volumetric strains neglects the importance of other mechanisms that could damage the structure and its surrounding utilities. Effective mitigation of the soil liquefaction hazard requires a thorough understanding of the potential consequences of liquefaction and the building performance objectives. The consequences of liquefaction, in turn, depend on site conditions, earthquake loading characteristics, and the structure. Hence, a rational design of site-specific liquefaction mitigation techniques requires a better understanding of the influence of these factors

[1] Postdoctoral Scholar, Dept. of Civil and Environ. Engrg., Univ. of Calif., Berkeley, CA 94702. Email: shideh@berkeley.edu
[2] Professor, Dept. of Civil and Environ. Engrg., Univ. of Calif., Berkeley, CA 94702. Email: bray@ce.berkeley.edu
[3] Professor, Dept. of Civil and Environ. Engrg., Univ. of Calif., Berkeley, CA 94702. Email: pestana@ce.berkeley.edu
[4] Associate Adjunct Professor, Dept. of Civil and Environ. Engrg., Univ. of Calif., Berkeley, CA 94702. Email: riemer@ce.berkeley.edu
[5] Associate Project Scientist, Center for Geotech. Modeling, Univ. of Calif., Davis, CA 95616. Email: dxwilson@ucdavis.edu

on the consequences of liquefaction.

Without a sufficient number of well-documented case histories, key parameters that affect soil and structural response need to be studied through carefully performed physical model tests. Accordingly, a series of centrifuge experiments were performed to generate model "case studies" of building response on liquefied ground. The soil response in the free-field was compared to that observed in the ground surrounding the structures, and the dominant mechanisms of settlement at different locations were identified. The key effects of different testing parameters were studied to advance the profession's understanding of liquefaction-induced settlement of buildings with shallow foundations. The centrifuge tests revealed the importance of the thickness and density of the liquefiable soil layer, the influence of spatial variations in transient hydraulic gradients, and the effects of ground motion characteristics and structural properties on building performance.

Centrifuge Testing Program

Four centrifuge experiments were performed to gain insight into the seismic performance of buildings with rigid mat foundations on a relatively thin deposit of liquefiable, clean sand. These experiments are described in more detail in Dashti 2009 and Dashti et al. 2010. Table 1 provides a summary of the centrifuge testing program. All units in this paper are provided in prototype scale. Centrifuge experiments were conducted at a spin acceleration of 55 g. The thickness (H_L) and the relative density (D_r) of the liquefiable layer as well as the contact pressure and Height/Width *(H/B*) ratio of the structural models were varied in the first three experiments to investigate the influence of key parameters affecting soil and structural response. The primary mechanisms involved in liquefaction-induced building settlement were identified in these experiments. The fourth experiment (T3-50) examined the influence of ground motion characteristics and the relative importance of key settlement mechanisms.

Figure 1 presents the model layout and instrumentation in experiment T3-30. The three tests referred to as T3-30, T3-50-SILT, and T3-50 included a liquefiable soil layer with a prototype thickness (H_L) of 3 m and nominal relative densities (D_r) of 30%, 50%, and 50%, respectively. In T3-50-SILT, the 2-m thick Monterey Sand placed on top of liquefiable Nevada Sand in the other experiments was replaced by a 0.8-m thick layer of silica flour underlying a 1.2-m thick layer of Monterey Sand. Test T6-30, with H_L = 6 m and D_r = 30%, provided information regarding the effects of the liquefiable layer thickness.

The lower deposit of uniform, fine Nevada Sand (D_{50} = 0.14 mm, $C_u \approx 2.0$, $e_{min} \approx 0.51$, $e_{max} \approx 0.78$) was dry pluviated to attain $D_r \approx 90\%$. The same Nevada Sand with an initial D_r of approximately 30% or 50% was then placed by dry pluviation as the liquefiable material. The hydraulic conductivities of Nevada Sand and silica flour are approximately 5×10^{-2} and 3×10^{-5} cm/s, respectively, when water is used as the pore fluid (Fiegel and Kutter 1994). A solution of hydroxypropyl methylcellulose in water was used as the pore fluid in these experiments with a viscosity of approximately 22(±2) times that of water (Stewart et al. 1998). The model was placed under vacuum and then flooded with CO_2 before saturation with the pore fluid. The phreatic surface was kept approximately 1.1 m below the ground surface.

All structural models were single-degree-of-freedom, elastic, flexible structures made of steel and aluminum placed on a 1 m-thick, rigid mat foundation. The base-line structure (A) represented a 2-story, stout building with a contact pressure of 80 kPa; a second structure (B) had an increased footing contact area but the same contact pressure; and a third structure (C) represented a taller 4-story building with increased bearing pressure (130 kPa). The fixed-base natural period of the structures ranged from 0.2 to 0.3 sec. Three structures similar to Structure A were used in T3-50 with different liquefaction remediation techniques. This paper only presents the response of the base-line structure (Structure A with no mitigation).

A series of realistic earthquake motions (Table 1) were applied to the base of the model consecutively in each experiment. Sufficient time between shakes was allowed to ensure full dissipation of excess pore pressures. Fig. 2 shows acceleration-time histories of two different ground motions that were used. The input motions included a sequence of scaled versions of the north-south, fault-normal component of the 1995 Kobe Port Island (P.I.) motion and a modified version of the fault-normal component of the ground motion recorded at the TCU078 station during the 1999 Chi-Chi Taiwan Earthquake with a peak base acceleration of 0.13 g.

Table 1. Centrifuge testing program

Test ID	**Liquefiable Layer Thickness/D_r**	**Structural Models**	**Input Ground Motion Characteristics**			
			Record	**PGA (g)**	**Significant Duration, D_{5-95} (s)**	**Arias Intensity, I_a (m/s)**
T6-30	6 m / 30%	Elastic buildings on rigid mat foundation (W x L x H): A: 6 x 9 x 5 m B: 12 x 18 x 5 m C: 6 x 9 x 9.2 m	Moderate Port Island (P.I.) 1995 Kobe	0.18	8	0.4
T3-30	3 m / 30%					
T3-50-SILT	3 m / 50%; with silt layer		Large P.I. 1995 Kobe	0.55	9	4.5
T3-50	3 m / 50%	Three similar elastic buildings on rigid mat foundation (W x L x H = 6 x 9 x 5 m)	Moderate P.I. 1995 Kobe	0.15	8	0.3
			TCU078 1999 Chi-Chi	0.13	28	0.6
			Large P.I. 1995 Kobe	0.38	11	2.7

Key Experimental Results

The average building vertical displacement-time histories in T6-30, T3-30, and T3-50-SILT during the large P.I. event are shown in Fig. 3. Average free-field displacement-time histories as well as the input ground motion (during T3-30) are also provided for comparison.

Fig. 4 presents the total head isochrones formed within the looser layer of Nevada Sand at key locations in T3-30 during the large P.I. event. Large vertical transient hydraulic gradients were formed in the free-field after about 1-2 sec of shaking. Free-field settlements occurred during strong shaking, which suggests that partial drainage occurred during shaking and the assumption of globally undrained loading is not valid in these experiments.

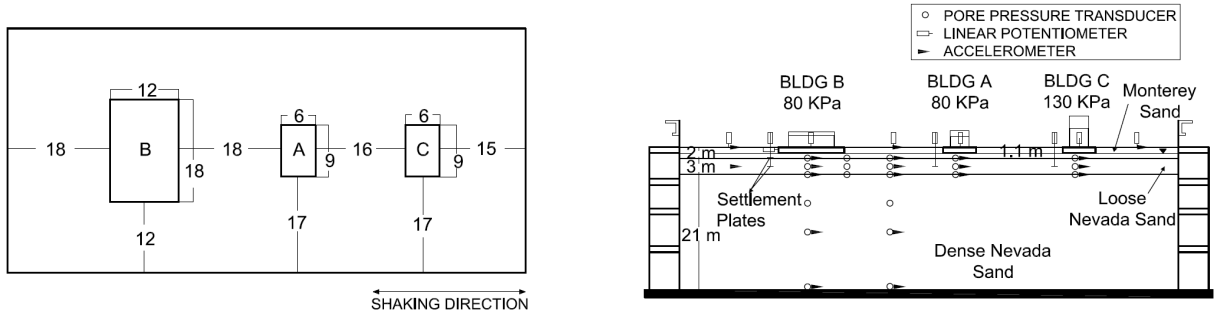

Figure 1. Centrifuge model layout in experiment T3-30: plan view (left) and cross section view (right). Most of the approximately 120 transducers are omitted for clarity. All dimensions are given in prototype scale in meters (Dashti et al. 2010).

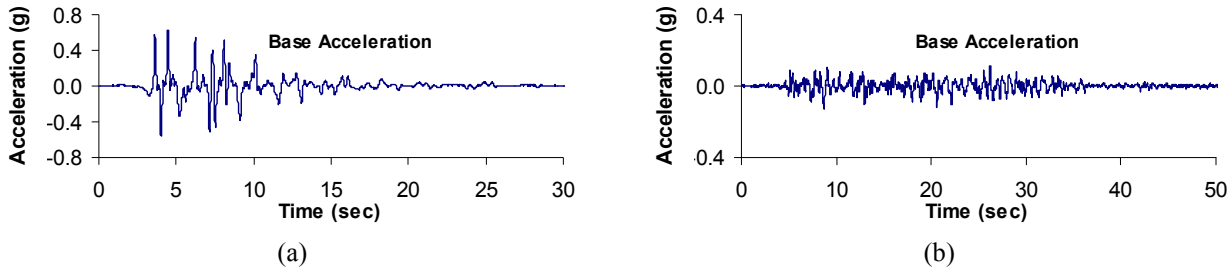

Figure 2. Input base acceleration-time histories: (a) large P.I. motion in experiment T6-30; (b) Chi-Chi TCU078 motion in experiment T3-50

Structures began settling after one significant loading cycle with a settlement rate that was roughly linear with time. Building settlements were shown to surpass quickly those measured in the free-field in all three experiments during this shake. Building settlement rates reduced dramatically after the end of strong shaking ($t \approx 12$ s) and became negligible at the end of shaking ($t \approx 25$ s). The observed trends suggest that the contribution of post-shaking reconsolidation settlements to the total building settlement must have been relatively minor in these experiments. A comparison of the flow potential in the two experiments indicated a stronger tendency for drainage and volumetric strains associated with drainage under structures during experiment T3-30 compared to T3-50-SILT. Yet, building settlements initiated similarly in all experiments. The apparent link between the initiation and intensity of shaking and the initiation and rate of building settlements points to the importance of cyclic inertial forces acting on the structure in its overall response. Additionally, the influence of partial drainage during earthquake shaking on the responses of the soil and structure should not be neglected.

Fig. 5 compares the settlement-time histories of the base-line structure (A) and soil surface in the free-field in experiment T3-50 during different earthquake scenarios. Arias Intensity-time histories of the input motions are shown as well. Arias Intensity (I_a) is an index representing the energy of the ground motion in units of *L/T* (Arias 1970) and defined as

$$I_a(T) = \frac{\pi}{2 \cdot g} \int_0^T a^2(t) \cdot dt \tag{1}$$

over the time period from 0 to T, where *a* = the measured acceleration value.

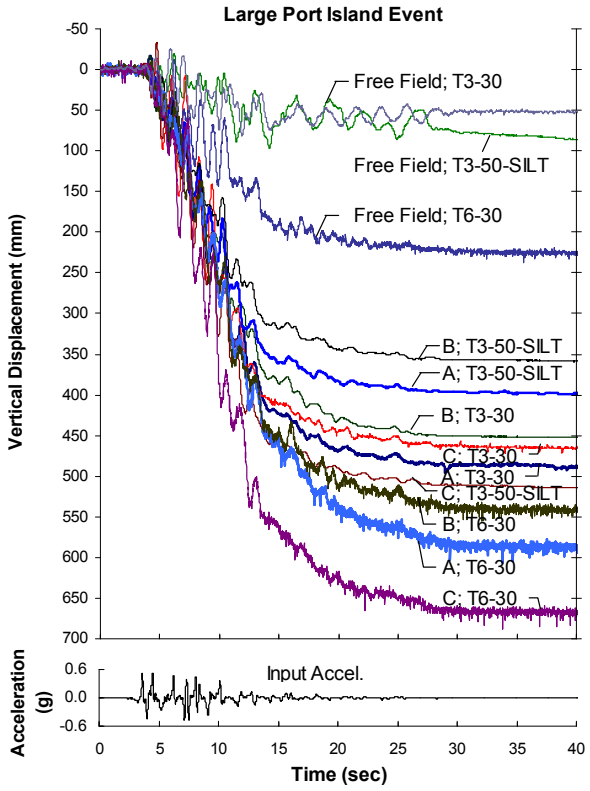

Figure 3. Settlement-time histories in T6-30, T3-30, and T3-50-SILT during the large P.I. event

The TCU078 motion was selected for its longer duration and slower rate of energy build-up compared to the P.I. motions. As shown in Fig. 5, the rate and duration of structural settlements observed during the TCU078 motion differed from those during the P.I. motion. Although the Arias Intensity and significant duration of the TCU078 event were respectively two and three times larger than those during the moderate P.I. event, structures settled less during the TCU078 earthquake. Therefore, even though a measure such as Arias Intensity describes many characteristics of a ground motion, it alone does not capture all of the potentially important effects of a ground motion on building settlement. Simpler ground motion measures, such as PGA and PGV, are even more deficient. Additional work is required to develop a more complete set of ground motion measures for this problem.

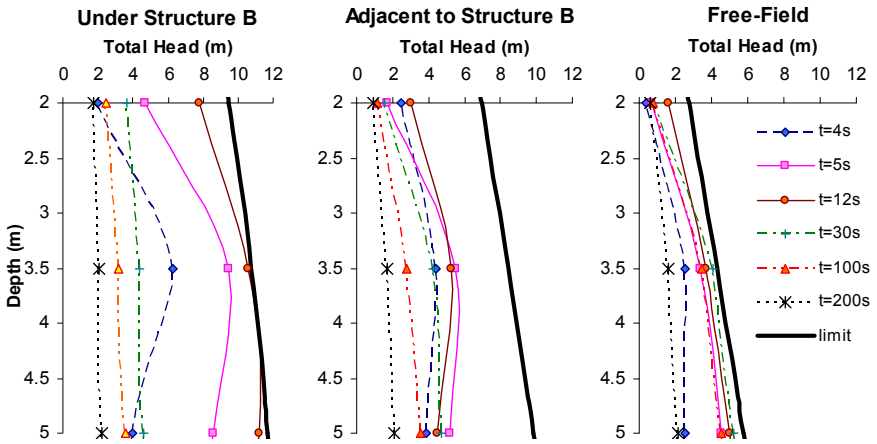

Figure 4. Representative total head isochrones measured in liquefiable soil under and adjacent to a structure and in the free-field in experiment T3-30 during the large P.I. event

Structure A settled as much or more than the free-field soil surface in each experiment, except during the TCU078 motion. Settlement of the lower dense deposit of Nevada Sand was negligible across the model during the TCU078 motion. The looser layer of Nevada Sand, however, developed large excess pore water pressures and experienced liquefaction in the free-field. Thus, relatively large volumetric strains were observed at locations away from the structures (free-field) due to particle sedimentation, consolidation, and drainage within the liquefiable layer. Smaller net excess pore pressures were measured within this layer under the buildings. These excess pore water pressures were too small to cause significant sedimentation, consolidation, volumetric strains due to localized drainage, or shear-type displacements due to partial bearing capacity failure under the buildings. As a result, structural settlements were mainly controlled by SSI-induced building ratcheting. The settlement mechanisms activated under the buildings were not sufficient to overcome the greater volumetric-type settlements within the liquefiable layer in the free-field. This resulted in the structures settling less than the free-field soil surface during this earthquake. These observations confirm that the pore water pressure response at key locations and the triggering and magnitude of various settlement mechanisms are controlled by the interacting effects of soil relative density, structural properties, and the rate at which ground motion energy is built-up.

Key Findings

The normalized average permanent building settlements measured during the large P.I. event in the first three centrifuge model tests are shown in Fig. 6. Results from available case histories and two previous centrifuge experimental studies are also included in this figure. The building settlements shown in Fig. 6 were estimated as the total settlement of structures minus the average settlement of the lower deposit of dense Nevada Sand during the corresponding earthquake. Settlements were then normalized by the initial thickness of the liquefying layer (H_L). The results of T6-30, where the liquefiable layer was relatively thick (i.e., H_L = 6 m), were consistent with the results from previous centrifuge tests and case histories involving deep deposits of liquefiable materials. The results of T3-30 and T3-50-SILT, where the liquefiable

layer was relatively thin (i.e., H_L = 3 m), were not consistent with other test results and observations. It appears that if there is a sufficient thickness of liquefiable soil present at a site, significant liquefaction-induced building settlements can occur that are not proportional to the thickness of the liquefying layer. These results indicate that normalizing building settlement by the thickness of the liquefiable layer is misleading in understanding the response of different structures founded on relatively thin, shallow deposits of saturated granular soils. Therefore, although Fig. 6 provides valuable insight, the use of normalized building settlements by the thickness of the liquefiable layer should be avoided in engineering practice. The results also highlight the need for a better understanding of the primary factors influencing liquefaction-induced building settlements.

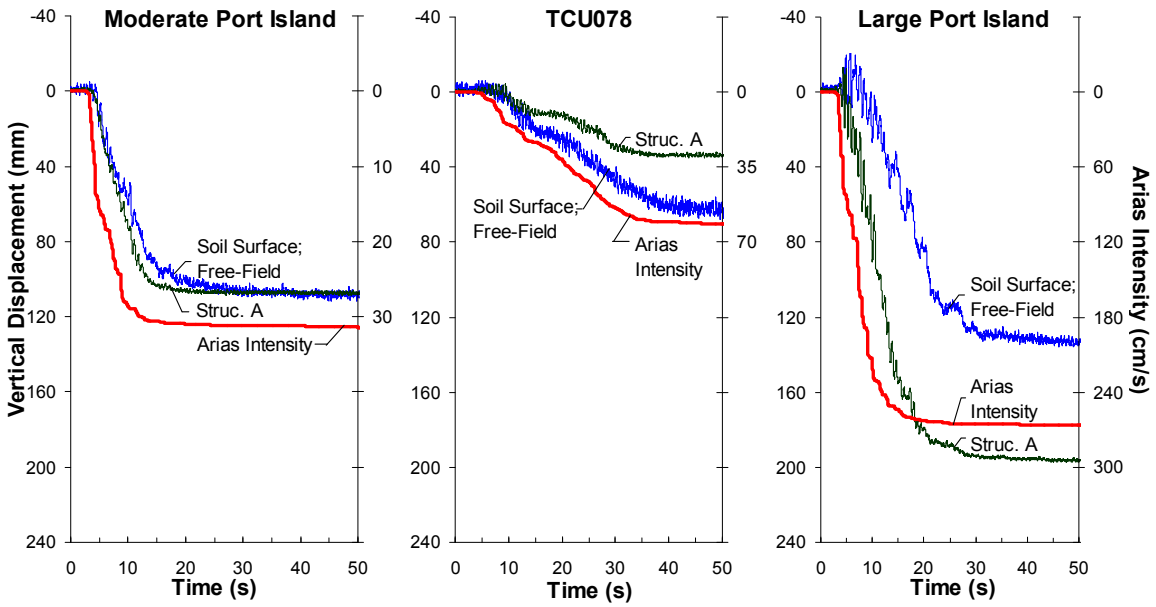

Figure 5. Vertical displacement of Structure A and the soil surface in the free-field in T3-50 with the Arias Intensity time history of the input motion during three earthquake scenarios

The primary settlement mechanisms identified in this study were (Dashti et al. 2010): (a) volumetric types: rapid drainage ($\varepsilon_{p\text{-}DR}$), sedimentation ($\varepsilon_{p\text{-}SED}$), and consolidation ($\varepsilon_{p\text{-}CON}$), and (b) deviatoric types: partial bearing capacity loss under the static load of the structure ($\varepsilon_{q\text{-}BC}$) and soil-structure-interaction (SSI) induced building ratcheting ($\varepsilon_{q\text{-}SSI}$). Although it is difficult to isolate and independently measure the effects of each mechanism, the separation of volumetric and deviatoric-induced settlements into these conceptual categories aids in understanding the sequence of liquefaction-induced building movements and the factors that contribute to them.

Significant transient hydraulic gradients developed soon after shaking began. They caused water to flow both within and out of the soil during shaking, which in turn produced volumetric strains in the soil ($\varepsilon_{p\text{-}DR}$). The contribution of this mechanism was greater during strong shaking when hydraulic gradients were greatest. The cyclic inertial forces acting on the structures worked them into the softened foundation soil ($\varepsilon_{q\text{-}SSI}$). SSI effects also amplified cyclic pore pressure-induced softening under the buildings, which further intensified other settlement

mechanisms. The generation of excess pore pressures reduced soil stiffness and strength under the foundation, which induced more static bearing-induced soil shearing ($\varepsilon_{p\text{-}BC}$). Static and dynamic deviatoric-induced movements ($\varepsilon_{q\text{-}BC}$ and $\varepsilon_{q\text{-}SSI}$) in combination with sedimentation ($\varepsilon_{p\text{-}SED}$) and localized volumetric strains due to partial drainage during earthquake shaking ($\varepsilon_{p\text{-}DR}$) were likely responsible for most of the building settlements measured in these experiments. Consolidation-induced settlement ($\varepsilon_{p\text{-}CON}$) also occurred during shaking, but its effects were most evident after strong shaking when there was insignificant generation of pore water pressures and net excess pore water pressures were able to dissipate. The relative contribution of these settlement mechanisms was shown to depend strongly on key parameters such as the liquefiable soil's relative density, the ground motion characteristics, building geometry and weight, and 3-D drainage capabilities.

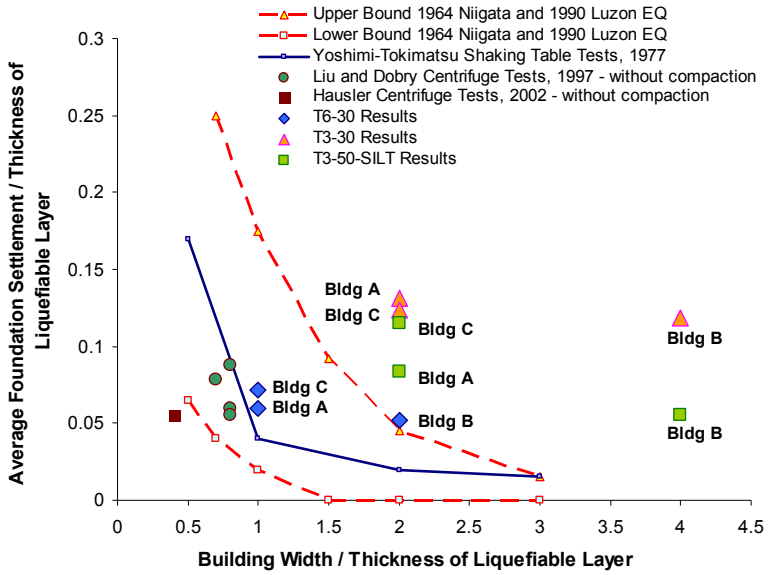

Figure 6. Normalized foundation settlements measured in the first three centrifuge experiments performed in this study during the large P.I. event compared to the available case histories and previous physical model tests (Dashti et al. 2010)

The settlement-time history of buildings during each earthquake appeared to follow the shape of the Arias Intensity-time histories of each motion (Fig. 5). The Arias Intensity of an earthquake motion depends on the intensity, frequency content, and duration of the motion, and its rate represents roughly the rate of earthquake energy build-up. This rate may be quantified by the Shaking Intensity Rate (*SIR*) as

$$SIR = I_{a5\text{-}75}/D_{5\text{-}75} \tag{2}$$

where $I_{a5\text{-}75}$ is the change in Arias Intensity from 5% to 75% of its total value during which it is approximately linear in these tests, and $D_{5\text{-}75}$ is its corresponding time duration. The *SIR* of a ground motion determines the rate of soil particle disturbance, excess pore pressure generation, seismic demand on structures, and the resulting SSI effects in the foundation soil. As a result, the initiation, rate, and amount of liquefaction-induced building settlement are expected to correlate

to *SIR*. By combining the effects of ground motion intensity, frequency content, and duration, the *SIR* of the ground motion better defines the seismic demand in terms of liquefaction-induced building settlement than the more conventionally used cyclic stress ratio (*CSR*).

The trends in the building settlement rate as a function of the shaking intensity rate (*SIR*) and the pre-event relative density (D_r) of the liquefiable soil are shown in Fig. 7. The presented results take into account the approximate change in the relative density of the liquefiable layer in each successive earthquake event. The level of shaking in these experiments is sufficient to induce liquefaction in the free-field. The results indicate that the rate of settlement increases as the motion *SIR* increases and as the soil D_r decreases. The apparent dependency of building settlement on *SIR* may allow *SIR* to be used in combination with other parameters in procedures that evaluate the consequences of liquefaction in the future.

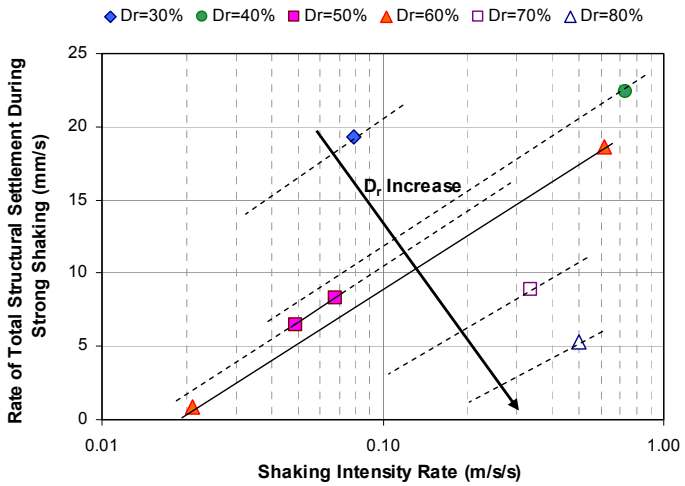

Figure 7. Trends in the initial settlement rate of Structure A in experiments with a 3 m-thick liquefiable sand (*SIR* = $Ia_{5\text{-}75}/D_{5\text{-}75}$)

Conclusions and Recommendations

Engineers often estimate liquefaction-induced building settlement using procedures developed to evaluate post-earthquake volumetric reconsolidation strains in the free-field. These procedures cannot capture liquefaction-induced building settlement, because they ignore partial drainage that occurs during strong shaking and the important deviatoric strain mechanisms that this testing program has shown to be important. Moreover, the centrifuge test results showed that building settlement is not proportional to the thickness of the liquefiable layer. Therefore, normalizing building settlements by the thickness of the liquefiable layer is misleading and should be avoided in engineering practice. There are currently no well-calibrated, simplified analytical tools available for estimating liquefaction-induced building settlements. The relative importance of various mechanisms of settlement has been shown to depend strongly on the properties of structure, underlying soil, and ground motion. Additionally, as most of the identified potentially critical mechanisms of seismically induced foundation settlement involve close coupling of cyclic pore water pressure generation and liquefaction, cyclic inertial forces,

and post-liquefaction residual strength, the assessment of total deformations is complex.

The seismic response of soil (containing a liquefiable stratum) and the overlying structure are evaluated typically through total stress analyses (Byrne et al. 2004). This approach, however, does not capture fundamental soil response, particularly when a structure is present, as it does not consider pore water pressures and SSI effects in the prediction of liquefaction. Instead, pore water pressures are indirectly accounted for in the reduced stiffness and strength values used after liquefaction is triggered. This approach is particularly misleading in predicting the consequences of liquefaction by not properly capturing the response and interaction of dominant mechanisms of settlement before and after liquefaction. A fully-coupled, dynamic, nonlinear, effective stress analysis of the problem that more accurately models SSI-induced shear stresses is recommended for a more reliable assessment of liquefaction triggering, post-liquefaction stability, and building settlement.

Acknowledgments

This material is based upon work supported by the National Science Foundation (NSF) under Grant No. CMMI-0530714. Any opinions, findings, and conclusions or recommendations expressed in this material are those of the authors and do not necessarily reflect the views of the NSF. Operation of the large geotechnical centrifuge at UC Davis is supported by the NSF George E. Brown, Jr. Network for Earthquake Engineering Simulation (NEES) program under Award No. CMMI-0402490.

References

Arias, A. (1970). "A measure of earthquake intensity." *Seismic design for nuclear power plants*, R. J. Hansen, ed., MIT Press, Cambridge, Mass.

Byrne, P. M., Park, S. S., Beaty, M., Sharp, M., Gonzalez, and L., Abdoun, T. (2004). "Numerical modeling of liquefaction and comparison with centrifuge tests," *Canadian Geotech. J.*, 41: 193-211.

Dashti, S. (2009). "Toward evaluating building performance on softened ground," *Ph.D. Dissertation*, University of California, Berkeley, Appendices I-IV.

Dashti, S., Bray, J.D., Pestana, J.M., Riemer, M.R. and Wilson, D. (2010). "Mechanisms of seismically-induced settlement of buildings with shallow foundations on liquefiable soil," *J. Geotech. Geoenviron. Engng*., ASCE, 136 (accepted for publication in 2010).

Fiegel, G.L., and Kutter, B.L. (1994). "Liquefaction-induced lateral spreading of mildly sloping ground," *J. Geotech. Eng.*, ASCE, 120(12), 2236-2243.

Hausler, E.A. (2002). "Influence of ground improvement on settlement and liquefaction: a study based on field case history evidence and dynamic geotechnical centrifuge tests." *Ph.D. Dissertation*, University of California, Berkeley, Ch. 5: 85-271.

Ishihara, K., and Yoshimine, M. (1992). "Evaluation of settlements in sand deposits following liquefaction during earthquakes," *J. Soils and Foundations*, 32(1), 173-188.

Liu, L. and Dobry, R. (1997). "Seismic response of shallow foundation on liquefiable sand," *J. Geotech. Geoenviron. Engng.*, ASCE, 123(6), 557-567.

Stewart, D.P., Chen, Y.R., and Kutter, B.L. (1998). "Experience with the use of methylcellulose as a viscous pore fluid in centrifuge models," *Geotechnical Testing Journal*, ASTM, 21(4), 365-369.

Tokimatsu K., and Seed H.B. (1987). "Evaluation of settlements in sands due to earthquake shaking," *J. Geotech. Engng.,* ASCE, 113(8), 861-878.